Gravitasi
Journal available at: https://bestjournal.untad.ac.id/index.php/GravitasiFisika
e-ISSN: 2654-4318 p-ISSN: 1412-2375

# Identification of Weak Zones in the Area of Sigi Regency Office Using Geoelectric Methods of Resistivity

**Sandra Sandra[2)]*. Sunaldi[1)], M. D. T. Musa[2)], Abdullah[2)], Muh. Rusydi[2)], Muh. Rusli[2)], Maskur[1)]**
[1)] Program Studi Fisika, Jurusan Fisika, Fakultas Matematika dan Ilmu Pengetahuan Alam, Universitas Tadulako
[2)] Program studi Teknik Geofisika, Jurusan Fisika, Fakultas Matematika dan Ilmu Pengetahuan Alam, Universitas TadulakoUniversity

**Information**

**Article history:**

Received: 29 May 2022

Accepted: 9 December 2022
Published: 23 December 2022

**Keywords:**
*Weak Zone,*
*Wenner Configuration*
*Resistivity*

**Abstract**

Research has been conducted with the title of identification of weak zones in the Sigi Regency office area using geoelectric methods of resistivity. The study aims to analyze the perlapission of subsurface rocks and determine the distribution of weak zones. The measurements were made on 15 track using the Wenner Configuration. The data obtained is calculated using Microsoft Excel and processed using the Res2Dinv 3.53 program that produce a cross-section of 2D resistivity. The results showed that the weak zone had resistance values of 20-180 Ωm which were suspected to be clay and sand. This weak zone is characterized by a low resistivity value and contrasting a large resistivity value compared to surrounding rocks. This weak zone is detected in almost all measurement trajectories of varying depth and is mostly at a depth of ± 6 m. The weak zone spreads southwest of the research site

*) e-mail: sandrafisika@gmail.com
DOI: 10.22487/gravitasi.v21i1.15909

## 1. INTRODUCTION

Bora Village, located in Sigi Biromaru District, is the capital of Sigi Regency, Central Sulawesi. As the capital of a developing regency, this area has office buildings such as the regent's office along with regional apparatus offices and other agencies. Along with the development of infrastructure development, this could potentially lead to an imbalance between the load of the building on the surface and the carrying capacity of the soil.

This imbalance has been seen in the damage to several office buildings such as the district head's office in the south [1]. This was exacerbated by the earthquake on September 28 2018 which resulted in damage to the office building and several parts of the building that collapsed. As the center of government and community services, this office building needs to be renovated while still considering its safety and comfort factors. This is to ensure the safety of government officials in serving the community. Therefore, before carrying out renovations, it is necessary to identify subsurface conditions.

Infrastructure development in an area needs to consider the carrying capacity of the soil. The building will be safe if the load does not exceed the carrying capacity of the soil. One of the factors that affect the carrying capacity of the soil is the existence of a weak zone. The weak zone is a condition below the earth's surface where there are areas that have a lower level of rock hardness than the surrounding area. Weak zones have high resistivity, because rocks that are more compact will more easily conduct current than rocks that are hollow, so that the resistivity value of compact rocks will be smaller. [2]. One method that can be used to identify weak zones is the resistivity geoelectric method [3].

The resistivity geoelectric method is a geophysical method that utilizes the nature of electric currents in the earth by detecting them above the earth's surface. Geoelectrical resistivity methods have also been used to identify weak zones, including by Fatoni et al [4] in the identification of weak zones on the Samarinda Bontang axis road using the Wenner Schlumberger Configuration geoelectric method. Wafi et al [5] have also used it in mapping weak zones using the Wenner Configuration geoelectric method and the Dutch Cone Penetrometer Test (DCPT). The purpose of this study was to analyze the subsurface rock layers and distribution of weak zones in the office area of Sigi Regency.

Based on the Geological Map of the Pasangkayu Sheet, the constituent rocks at the study site and its surroundings are the Pakuli Formation, Wana Complex and Alluvium consisting of clay, sand, gravel, conglomerate, sandstone, genes and quartzite (Figure 1).

The resistivity geoelectric method is one of a group of geoelectrical methods that can be used to study subsurface conditions by studying the nature of electric currents in rocks beneath the earth's surface. The discussion of the electricity of the earth, in accordance with its nature tends to discuss the electrical properties of the earth. The resistivity geoelectrical method is a geoelectrical method that studies the resistivity properties of rock layers in the earth [6].

Resistance is a quantity that indicates the level of resistance to the electric current of a material. The approach used to obtain the resistivity value of a medium below the earth's surface is by assuming that the earth is an isotropically homogeneous medium [7]. From this assumption, the measured resistance is the actual resistivity without having to depend on the spacing of the electrodes. But in reality, the earth is composed of layers with different resistivity values, so the measured potential is the effect of these layers. This causes the measured resistivity value to appear to be the resistivity value for only one layer. But in reality, what is actually measured is the apparent resistance (ρa) [8].

According to Hurun [9], the magnitude of the apparent resistivity (ρa) (ohm-m) is:

$$\rho_a = \frac{2\pi}{\left[\left(\frac{1}{r_1}-\frac{1}{r_2}\right)-\left(\frac{1}{r_3}-\frac{1}{r_4}\right)\right]} \frac{\Delta V}{I} \quad (1)$$

or

$$\rho_a = K \frac{\Delta V}{I} \quad (2)$$

where

$$K = \frac{2\pi}{\left[\left(\frac{1}{r_1}-\frac{1}{r_2}\right)-\left(\frac{1}{r_3}-\frac{1}{r_4}\right)\right]} \quad (3)$$

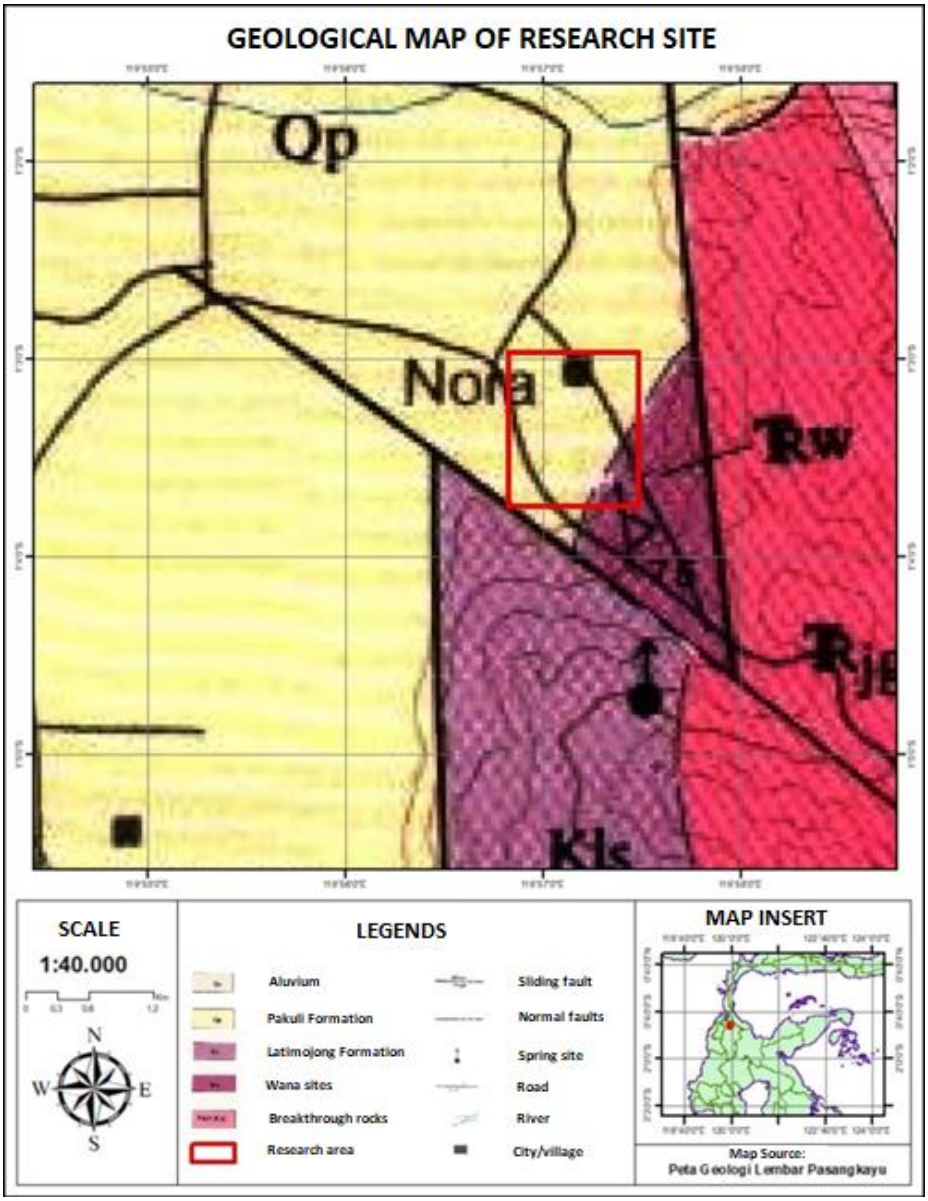


**Figure 1.** Geological Map

The Wenner configuration is a type of configuration in geoelectrical exploration which has a sequence of electrodes arranged in a track symmetrically about the center point. Electrodes in the Wenner Configuration have good vertical resolution, where sensitivity to lateral changes is high but weak to current penetration with depth [10]. The arrangement of the Wenner Configuration electrodes can be seen in Figure 2.

According to Badaruddin [11], the limit of enlargement of the electrode spacing depends on the ability of the tool used. The more sensitive and the greater the current that can be generated, the greater the spacing that can be measured, so that the deeper layers are detected. Due to the property that an increase in the current electrode distance is followed by an increase in the potential electrode distance, the Wenner Configuration can detect local inhomogeneity from the observed location. The choice of spacing depends on the depth to be mapped.

The Wenner Configuration geometry factor can be derived by using the equation:

$$\rho = \frac{2\pi}{\left(\frac{1}{C_1P_1}-\frac{1}{C_2P_1}-\frac{1}{C_1P_2}+\frac{1}{C_2P_2}\right)}\frac{\Delta V}{I} \quad (4)$$

where

$$K = \frac{2\pi}{\left[\left(\frac{1}{r_1}-\frac{1}{r_2}\right)-\left(\frac{1}{r_3}-\frac{1}{r_4}\right)\right]} \quad (5)$$

or

$$K = 2\pi a \quad (6)$$

Thus,

$$\rho = K\frac{\Delta V}{I} \quad (7)$$

## 2. MATERIALS AND METHODS

The research location is in the office area of Sigi Regency, Bora Village, Sigi Biromaru District, Sigi Regency, Central Sulawesi Province. Geographically, the research location is located at coordinates 19°56'50.16"-119°57'22.02" East Longitude and 1°3'8.38"-1°3'41.87" South Latitude. An overview of the research location can be seen in Figure 3.

Retrieval of data using the resistivity geoelectric method with the following tools and materials: One unit of geoelectrical resistivity measuring instrument. GPS, Geological compass, Meter, Hammer, Writing tools and tables.

Data collection in the field consists of 15 tracks that begin with determining the position of the measuring point, and the direction of the track and measuring its direction using GPS, making a stretch in the form of a straight line with a length of 100 m, plugging in the electrodes with an electrode spacing of 5 m, laying out the wires and connecting the wires to the electrodes, assembling the resistivity geoelectric device and taking measurements. The data obtained in the field are current, potential and spacing.

The data obtained is then inputted into Microsoft Excel, then calculating the geometry factor value using equation (6) and the apparent resistivity using Equation (7). The data is then processed using the Res2Dinv program. The results obtained from the inverse program are in the form of variations in the value of resistivity, depth and layer thickness which are then analyzed and interpreted. To obtain more accurate interpretation results, supporting data related to the conditions of the study area are needed, including geological maps, tables of rock type resistance values and results of previous research around the study area.

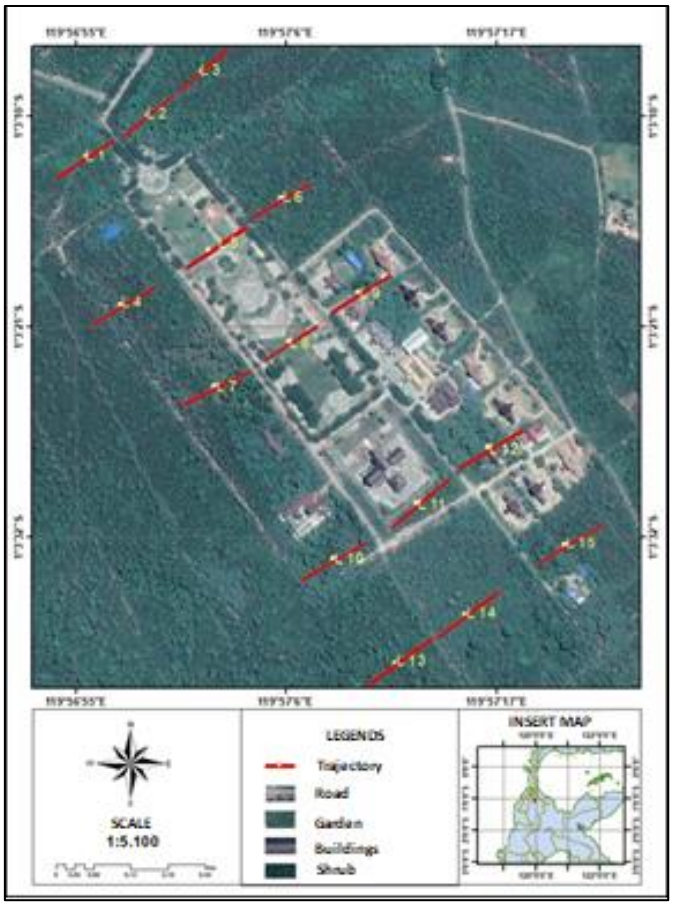


**Figure 2.** Map of the research area

## 4. RESULTS AND DISCUSSION

The measured data were then processed using the Res2Dinv program to obtain a cross-sectional model of the resistivity. This program generates 3 2D cross-sections of resistivity. The first cross-section shows the measured apparent resistivity cross-section, the second cross-section shows the calculated apparent resistivity cross-section and the third cross-section shows the inverse resistivity section obtained through the inversion modeling process.. The model obtained through the inversion process was iterated several times to reduce the existing root mean squared error (RMS) value. The inverted data shows variations in the resistivity value (ρ) and the depth of each layer.

Following table is the results of data processing for each track:

**Table 1.** Data processing results

| Track | Resistivity (Ωm) | | Error (%) |
|---|---|---|---|
| | Minimum | Maxsimum | |
| 1 | 33,32 | 449,16 | 2,6 |
| 2 | 23,68 | 440,17 | 3,2 |
| 3 | 22,36 | 389,98 | 4,2 |
| 4 | 28,42 | 724,51 | 3,2 |
| 5 | 32,74 | 388,95 | 3,2 |
| 6 | 41,30 | 663,11 | 3,6 |
| 7 | 49,36 | 739,66 | 5,2 |
| 8 | 56,64 | 816,92 | 2,8 |
| 9 | 34,77 | 609,77 | 4,8 |
| 10 | 83,96 | 1230,50 | 5,0 |
| 11 | 68,11 | 521,14 | 3,8 |
| 12 | 26,78 | 273,92 | 2,7 |
| 13 | 98,56 | 1077,40 | 3,9 |
| 14 | 97,45 | 640,66 | 2,8 |
| 15 | 63,98 | 520,80 | 2,7 |

To obtain the distribution of weak zones, the measurement path is divided into 5 consisting of Tracks a, b, c, d and e. The cross-section of the type of barriers for each lane can be seen as follows:

1. Track a

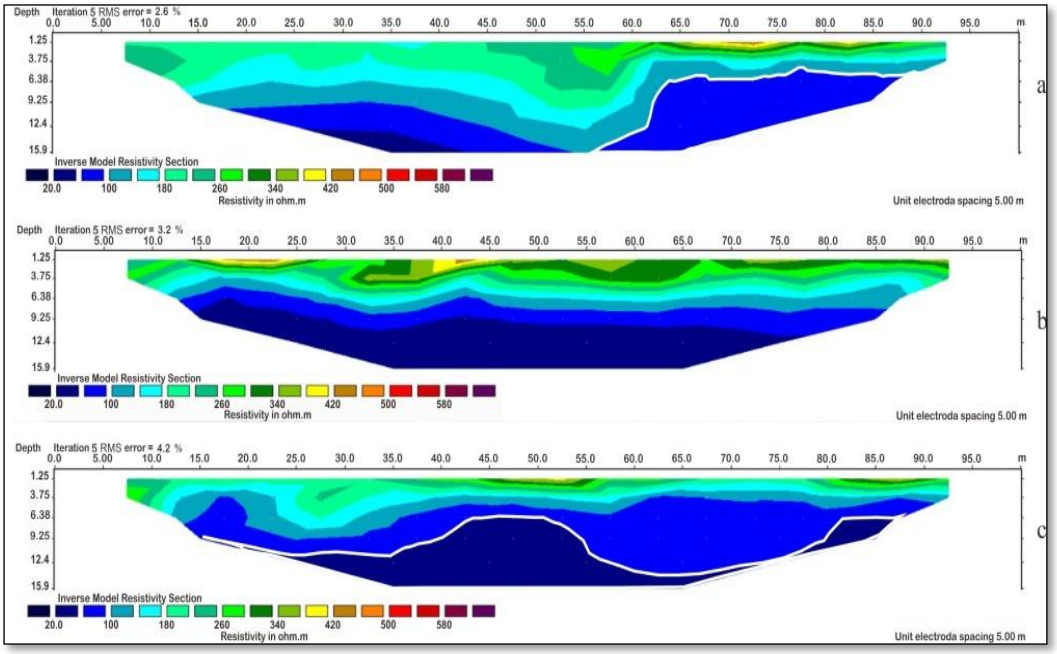


**Figure 4.** Cross section of the obstacle type a (a) Track 1, (b) Track 2 and (c) Track 3

Track a is in the northwest direction of the research location consisting of Track 1, Track 2 and Track 3. The three Tracks are in a straight line with the distance between Tracks 1 and 2 as far as 41 m and the distance between Tracks 2 and 3 as far as 24 m. The processing results can be seen in Figure 4. On track 1, a weak zone is visible on the 55-90 m meter which is suspected to be a layer of sand at a depth of ± 6-15 m bmt with a resistivity value of < 100 Ωm. On track 2 no weak zone is detected. Furthermore, on track 3 a weak zone was detected at meter 15-88 m which was suspected to be a layer of clay from a depth of ± 6-15 m bmt with a resistivity value of < 60 Ωm. The weak zone on Track a spreads northeast.

2. Track b

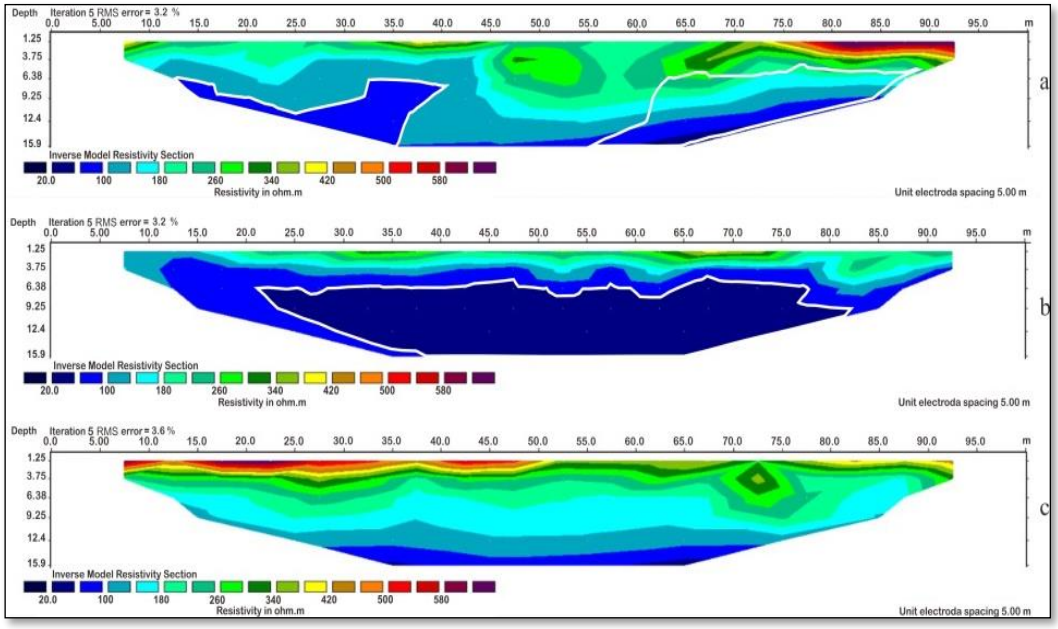


**Figure 5.** Cross section of the obstacle type b (a) Track 4, (b) Track 5 and (c) Track 6

Track b is in the northwest of the research location after Track a. This track consists of Track 4, Track 5 and Track 6. The three Tracks are in a straight line with the distance between Tracks 4 and 5 as far as 83 m and the distance between Tracks 5 and 6 as far as 40 m. The processing results can be seen in Figure 5. On track 2, a weak zone is visible on the 13-38 m meter which is suspected to be a layer of sand at a depth of ± 3 m bmt with a resistivity value of < 100 Ωm. On track 5 a weak zone is detected at meter 21-83 m which is suspected to be a layer of clay at a depth of ± 6-12 m bmt with a resistivity value of < 60 Ωm. Furthermore, on Track 6 no weak zones were detected. The weak zone on Track b spreads southwest.

3. Track c

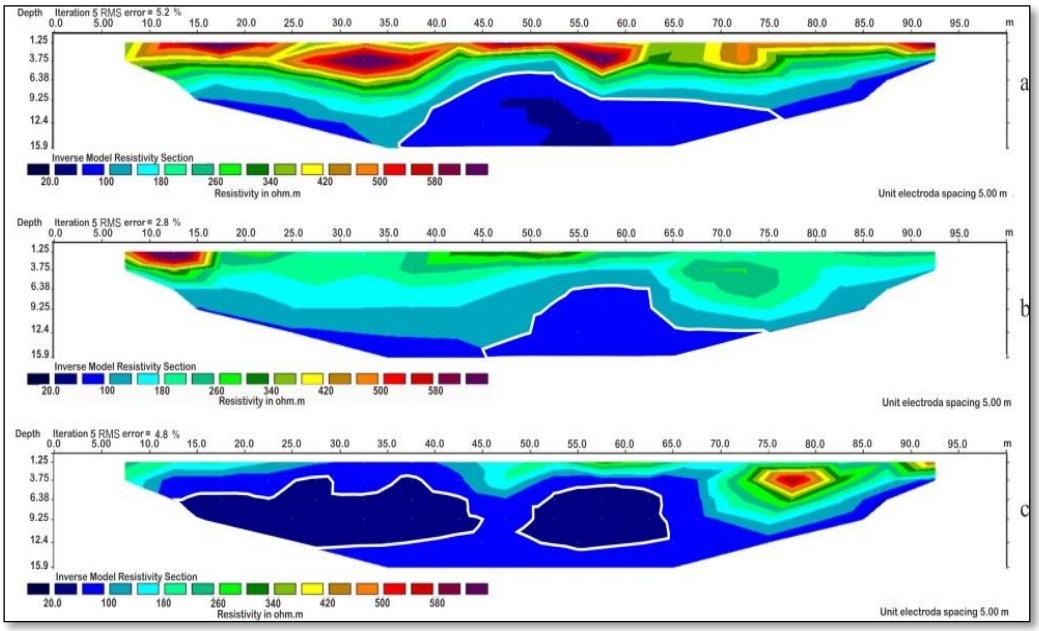


**Figure 6.** Cross section of the obstacle type c (a) Track 7, (b) Track 8 and (c) Track 9

Track c is in the middle of the research location consisting of Track 7, Track 8 and Track 9. The three Tracks are in a straight line with the distance between Tracks 7 and 8 as far as 52 m and the distance between Tracks 8 and 9 as far as 36 m. Processing results can be seen in Figure 6. On track 7, a weak zone is visible on the 36-75 m meter which is suspected to be a layer of sand at a depth of ± 6-10 m bmt with a resistivity value of < 100 Ωm. On track 8 a weak zone is detected at meter 50-65 m which is suspected as a layer of sand at a depth of ± 6-15 m bmt with a resistivity value of < 100 Ωm. Furthermore, on track 9 a weak zone was detected at meters 13-44 m and 48-65 m which was suspected to be a layer of clay at a depth of ± 3-12 m bmt with a resistivity value of 60 Ωm. Weak zones on Track c are detected in all Tracks and spread to the southwest.

4. Track d

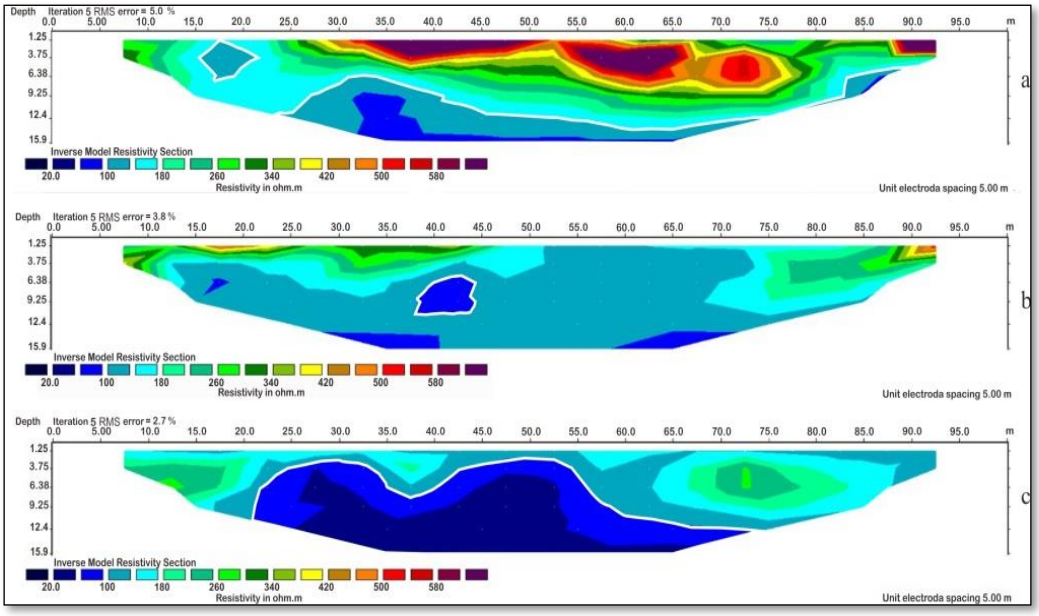


**Figure 7.** Cross section of the obstacle type d (a) Track 10, (b) Track 11 and (c) Track 12

Track d is in the southeast of the research location after track c. This track consists of Tracks 10, Tracks 11 and Tracks 12. The three Tracks are in a straight line with the distance between Tracks 10 and 11 as far as 65 m and the distance between Tracks 11 and 12 as far as 41 m. The results of the processing can be seen in Figure 7. On track 10 you can see a weak zone at 15-22 m and 81-90 m which is close to the ground surface. This weak zone is suspected as a layer of sand with a resistivity value of <140 Ωm. On track 11, a weak zone is detected at meter 37-44 m which is suspected to be a layer of sand at a depth of ± 6 m bmt with a resistivity value of 100 Ωm. Furthermore, on track 12 a weak zone was detected at meter 25-65 m which was suspected to be a layer of clay at a depth of ± 3-14 m bmt with a resistivity value of <100 Ωm. The weak zone in Lane d is spread across all Passages and spreads northwest.

5. Track e

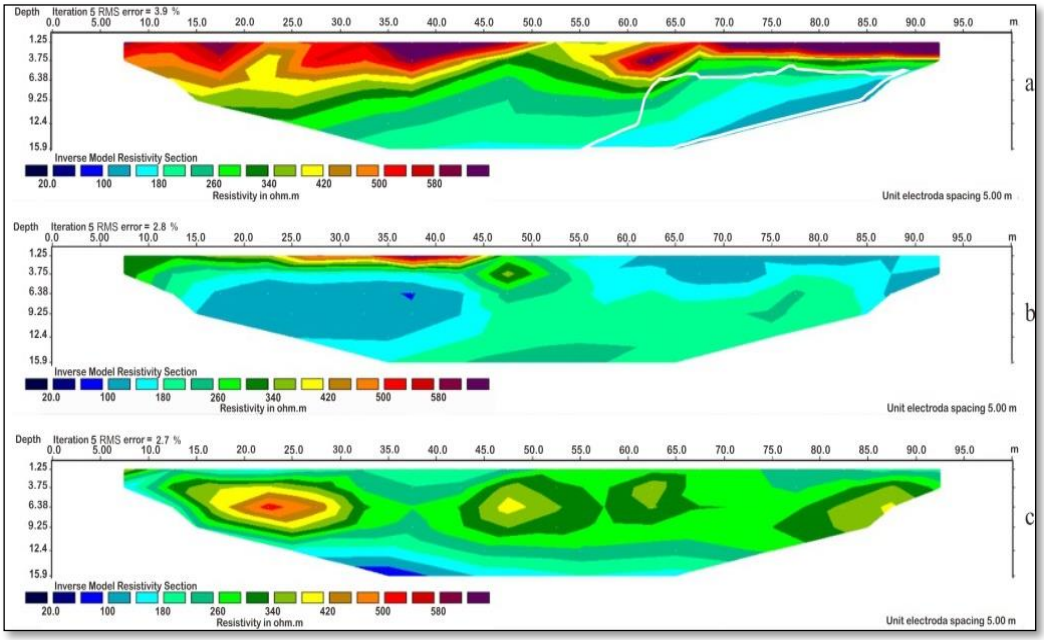


**Figure 8.** Cross section of the obstacle type e (a) Track 13, (b) Track 14 and (c) Track 15

Track e is at the southeastern end of the research location consisting of Tracks 13, Tracks 14 and Tracks 15. The three Tracks are in a straight line with the distance between Tracks 13 and 14 as far as 28 m and the distance between Tracks 14 and 15 as far as 95 m. Processing results can be seen in Figure 8. On track 13, a weak zone is seen at the 55-90 m meter which

is suspected to be a layer of sand at a depth of ± 6-15 m bmt with a resistivity value of < 180 Ωm. On track 14, a weak zone is detected at meter 12-45 m which is suspected as a layer of sand at a depth of ± 3 m bmt with a resistivity value of < 180 Ωm. The weak zone is again visible at 55-90 m which is close to ground level. Furthermore, on Track 15 no weak zones were detected. The weak zone in Track e spreads southwest of the study location.

Based on the results of the interpretation of all 2D cross-sections, it can be seen that the layers are arranged and the presence of layers that are suspected as weak zones in almost all measurement paths. Weak zones were detected at varying depths between 3-15 m bmt with a distribution towards the southwest of the study location. This zone has a resistivity value of 20-180 Ωm which is thought to consist of clay and sand and is characterized by a low resistivity value and a large resistivity contrast compared to the surrounding rock. This is in accordance with Anjarsari's research [12] that analyzed the relationship between seismic and geotechnical data in the Sigi Regional government office area stating that in the southwestern part of the Sigi Regency office area there is a heavy level of damage to the building structure where the section has a low shear wave propagation. This shows that the subsurface rocks consist of rocks that are not compact (weak zone).

## 5. CONCLUSION

Based on the research results, a weak zone consisting of clay and sand is obtained which has a resistivity value of 20-180 Ωm. This zone is characterized by low resistivity values and large resistivity contrast compared to the surrounding rocks. The weak zone was detected to spread at depths varying between 3-15 m bmt with a spread towards the southwest of the study location. Weak zones found in the study area are interpreted as rocks that are soft and not compact, so there is a risk of not being able to withstand structural changes due to the pressure of gravity from the buildings above it.

## REFERENCES


[1] Hadi, W. (2015). *Perkantoran Pemkab Sigi di Desa Bora Rusak. Diperoleh dari website Kompasiana*: https://www.kompasiana.com/h.wijaya/55485ae4547b618a1625256f/perkantoran-pemkab-sigi-di-desa-bora-rusak. Diakses 22 Januari 2022.

[2] Dani, I., Sinambela, R. Z., dan Yogi, I. B. S. (2020). Rekonstruksi Penampang Zona Rawan Longsor di Daerah Pidada, Bandar Lampung, Menggunakan Metode Tomografi Seismik Refraksi. *Prosiding SINTA* 3 (2020) (hal 1-5). Bandar Lampung: Jurusan Teknik Geofisika Universitas Lampung.

[3] Makmur, S., Sehah, dan Sugito. (2016). Analisis Zona Lemah (Amblesan) di Kawasan Jalan Raya Gunung Tugel Kabupaten Banyumas Berdasarkan Survei Geolistrik Konfigurasi Wenner. *Techno*. *17*(2), 111-121.

[4] Fatoni, A. R., Supriyanto, dan Lazar, P. AD. (2021). Identifikasi Zona Lemah di Jalan Poros Samarinda Bontang dengan Menggunakan Metode Geolistrik Konfigurasi Wenner Schlumberger. *Jurnal Geosains Kutai Basin*, *4*(1), 1-7.

[5] Wafi, A., Santosa, B. J., dan Warnana, D. D. (2013). Pemetaan Zona Lemah Menggunakan Metode Geolistrik Konfigurasi Wenner dan Dutch Cone Penetrometer Test (Dcpt). *Jurnal Sains dan Seni POMITS*, *2*(1), 92-95.

[6] Telford, W. M., Geldart, L.P., *and* Sheriff, R. E. (1990). *Applied Geophysics Second Edition*. New York: Cambridge University Press.

[7] Bahri. (2005). *Hand Out Mata Kuliah Geofisika Lingkungan dengan Topik Metode Geolistrik Resistivitas*. Surabaya: ITS.

[8] Reynolds, J. M. (1997). *An Introduction to Applied and Environmental Geophysics*. England: John Wiley and Sons.

[9] Hurun, N. (2016). Analisis Data Geolistrik Untuk Pemodelan Struktur Geologi Bawah Permukaan Gunung Lumpur Bangkalan. *Skripsi*. Fakultas Sains dan Teknologi, Universitas Islam Negeri Maulana Malik Ibrahim. Malang.

[10] Hakim dan Manrulu, R. M. (2016). Aplikasi Konfigurasi Wenner Dalam Menganalisis Jenis Material Bawah Permukaan. *Jurnal Ilmiah Pendidikan Fisika Al-BiRuNi*, *05*(1), 95-103. DOI: 10.24042/jpif albiruni.v5i1.109.

[11] Badaruddin. (2017). Penyelidikan Lapisan Batuan Dengan Metode Geolistrik Di Wilayah Balingara Kecamatan Ampana Tete Kabupaten Tojo Una-Una Sulawesi Tengah. *Gravitasi*, *15*(1),1-4. DOI: 10.22487/gravitasi.v15i1.7993.

[12] Anjarsari, R. (2022). Analisis Hubungan Data Seismik dan Geoteknik di Area Perkantoran Pemerintah Daerah Sigi. *Skripsi*. Fakultas Matematika dan Ilmu Pengetahuan Alam. Universitas Tadulako. Palu.